ELSEVIER

Biochimica et Biophysica Acta 1196 (1994) 131–138

BBA Biochimica et Biophysica Acta

An analysis of cardiac sodium channel properties using digital signal processing techniques

David A. Saint *, Michael K. Pugsley, Shin-Ho Chung

Protein Dynamics Unit, Department of Chemistry, Australian National University, Canberra, ACT 2601, Australia

Received 26 April 1994

Abstract

The properties of single sodium channels in membrane patches from isolated rat ventricular myocytes were analyzed. Both cell-attached and inside-out patch configurations were examined. A digital signal processing method was used which allowed accurate determination of single-channel conductance and mean open time, even in situations where many channels coexisted in the patch. The results show that the cardiac sodium channel has a conductance of 5.3 pS at room temperature, and shows no rectification or saturation in the physiological ranges of ion concentration and membrane potential. The active channels contained in the membrane patch opened and closed independently of each other. A transition probability matrix, which describes transitions between all current levels, can also be generated, analysis of which permits an estimate of individual mean channel open time as well as the degree of coupling between channels.

Keywords: Cardiac sodium ion channel; Sodium ion channel; Single channel; Digital signal processing technique; Hidden Markov Model processing

1. Introduction

There is currently some controversy regarding the properties of cardiac sodium channels. Several different estimates of the single-channel conductance have been given [1–3], and the presence or absence of subconductance states seems to be unresolved [4]. A major problem encountered in the analysis of cardiac sodium channels, which open in response to an appropriate change in membrane potential, is the comparatively rapid kinetics of activation and inactivation, in contrast to the situation with ligand gated channels that generally have a constant open probability over time. In addition, in most experimental situations several sodium channels co-exist in the membrane patch. In combination with the rapid transient increase in open probability this leads to the channels piling up, leading to the coincidental opening of many channels. This makes analysis of underlying individual single-channel properties very difficult. To circumvent these difficulties, a common strategy has been to use agents which remove inactivation of the channels, such as brevitoxin [5] or DPI [6,7]. However, one can never be sure that channel properties other than inactivation are not affected by the toxin, in particular the open state conductance and the presence or absence of sub-conductance states. Indeed alterations of sodium channel conductance by the commonly used toxin, batrachotoxin, have recently been documented [8].

An unambiguous measure of single-channel conductance, and whether rectification or saturation is present, is of course essential if one is to develop meaningful models of ion permeation through the channel. Related to this is the question of whether the ion conducting pathways show any degree of cooperativity, and whether they can assume open states with more than one conductance level. With this in mind we have analysed cardiac sodium channels unmodified by toxins, using a digital signal processing technique based on a hidden Markov model [9,10]. This approach, often referred to as the HMM technique, was initially developed as an analysis technique applicable to channels not displaying time-dependent changes in transition probabilities such as those caused by inactivation or desensitisation [11,12]. Here we report an extension of this technique to encompass an analysis of channels with rapid (and voltage-dependent) kinetics, as applied to cardiac sodium channels. The resulting data gives a single-channel conductance for the cardiac sodium channel of 5.3 pS ± 0.2 pS at room temperature, with no obvious subconductance

* Corresponding author. E-mail: David.Saint@anu.edu.au. Fax: +61 6 2472792.

SSDI 0005-2736(94)00206-1

states. The channel does not rectify or saturate in the physiological ranges of ion concentration or membrane potential, and the conductance increases as expected with higher sodium ion concentrations. The data also shows that, even when many channels coexist in the patch, they behave predominantly independently of each other at all voltages, displaying a coupling coefficient of essentially zero. Mean single-channel open time estimates using this technique were in close agreement with estimates from other techniques.

2. Methods

2.1. Isolation of cardiac myocytes

Enzymatic isolation of cardiac myocytes was performed according to the method of Farmer [13]. Male Wistar rats (300–350 g) were given an injection of heparin (2000 units i.p.) and killed by cervical dislocation 25 min later. Hearts were removed, washed in an ice-cold, oxygenated, calcium-free Tyrode's solution for 5 min before being perfused, via an aortic cannula, with the same calcium-free Tyrode's solution warmed to 37°C at a perfusion rate of between 9 and 10 ml min^{-1}. This facilitated the removal of blood from both the coronary vasculature and ventricular chambers. The Tyrode's solution contained in mM: NaCl, 134; Tes (*N*-tris(hydroxymethyl)methyl-2-aminoethanesulfonic acid), 10; KCl, 4; $MgCl_2$, 1.2; NaH_2PO_4, 1.2; D-glucose, 11, and was adjusted to pH 7.4 with 1.0 M NaOH. After 5 min of wash the heart was subjected to enzymatic dissociation in 25 μM calcium Tyrode's solution containing proteinase (0.1 mg ml^{-1}, Sigma Type XIV), collagenase (1 mg ml^{-1}, Worthington CLS II), and fetal calf serum (1 μg ml^{-1}).

Approximately 35–40 min later the heart became pale and flaccid. The ventricles were removed in one-third sections. Each section was cut into small pieces in fresh 25 μM calcium-Tyrodes solution and triturated to dissociate myocytes. Cell suspensions were then centrifuged and washed in a 200 μM calcium-Tyrode's solution. Finally the cells were resuspended in Tyrode's solution containing 1 mM calcium and approx. 1 h later plated onto glass coverslips. All cells were prepared and stored at room temperature (20–22°C).

2.2. Solutions and drugs

Unless stated otherwise, all experiments were performed at room temperature (20–21°C) in a bath solution containing (mM): K^+-aspartate, 140; EGTA, 10; $MgCl_2$, 2.0; $CaCl_2$, 1; Tes, 10; ATP (disodium salt), 10; pH adjusted to 7.4 with 1.0 M KOH. The membrane potential of the cells in this solution is essentially zero. The pipette solution contained (mM): NaF (or NaCl), 140; Tes 10; pH adjusted to 7.4 with NaOH.

2.3. Data recording and processing

Electrodes were prepared from borosilicate glass using a two-stage puller and resistances were typically 1–5 MΩ when they were filled with the pipette solution. Current recording was performed using an Axopatch 200 A amplifier (Axon Instruments). Voltage pulse protocols were generated by a computer, and the resulting current records were digitised with a 12 bit analogue-to-digital converter and stored on the computer hard disk for subsequent analysis. Current records were filtered at 5 kHz and sampled at 10 kHz.

Accurate capacitative transient cancellation is essential for the analysis technique to be successful, and this was done off-line using software written for the purpose. After recording many trials, usually 100 or 200, of a given voltage protocol (generally a voltage step to a potential in the range of −60 mV to 0 mV from a pre-pulse potential of −150 mV) several records were made of the current resulting from a voltage step of the same magnitude, but over a range of voltage which did not activate any channel activity (typically −60 mV to +50 mV). At this pre-pulse potential all sodium channels are inactivated. This capacitative current was averaged over 9 or 10 trials, and the resulting template subtracted from the original trials which did contain channel activity. This approach relies on the assumption that the membrane capacitance is the same at different voltages, an assumption which seems valid since this procedure generally gave an essentially flat baseline. Sections of each record containing channel activity were then excised from the records and concatenated into a data file containing the entire record of channel activity at a given voltage. This procedure was repeated for each experimental protocol. The resulting data files were then analysed using digital signal processing techniques. The output from this analysis is in the form of a signal estimate which gives the number of current levels in the record, the actual values of these levels, and transition probabilities between all levels. Examination of the transition probability matrix yields the mean open time and the coupling co-efficient for the channels. Information on the existence of sub-conductance states can also be derived from the transition probability matrix (see Results). The transmembrane potential we quote refers to the potential at the inner surface of the membrane with respect to the outer surface of the membrane. Inward currents are displayed as upward deflections.

3. Results

3.1. Accurate determination of single-channel conductance

Fig. 1 illustrates the analysis technique. The four current traces in Fig. 1A show examples of the original records obtained when the potential across a cell-attached

membrane patch was stepped from a conditioning potential of −150 mV to −50 mV. Small amplitude single-channel currents can just be discerned, but they are largely obscured by the prominent capacitative current transient. The same records after subtraction of the capacitative current template are shown in Fig. 1B. These records have an essentially flat baseline apart from a slight residual transient due to amplifier saturation at the peak of the capacitative current. The section of data between the dotted lines was then excised from each record and appended to a continuous data file, which normally consisted of 100 to 200 such records. The section of such a data file generated by the four traces shown is illustrated at a higher gain in Fig. 1C. We refer to this data record as the concatenated data file.

To determine the conductance levels of channel currents, we assumed that the signal sequence in this concatenated data file can be represented as a first-order Markov chain with 100 possible signal levels. Using this signal model, we then obtained the maximum a posteriori (MAP) estimate of the signal sequence, according to the processing method detailed elsewhere [9,10]. The original concatenated data file is shown in the upper panel of Fig. 2A, with the corresponding MAP signal sequence shown in

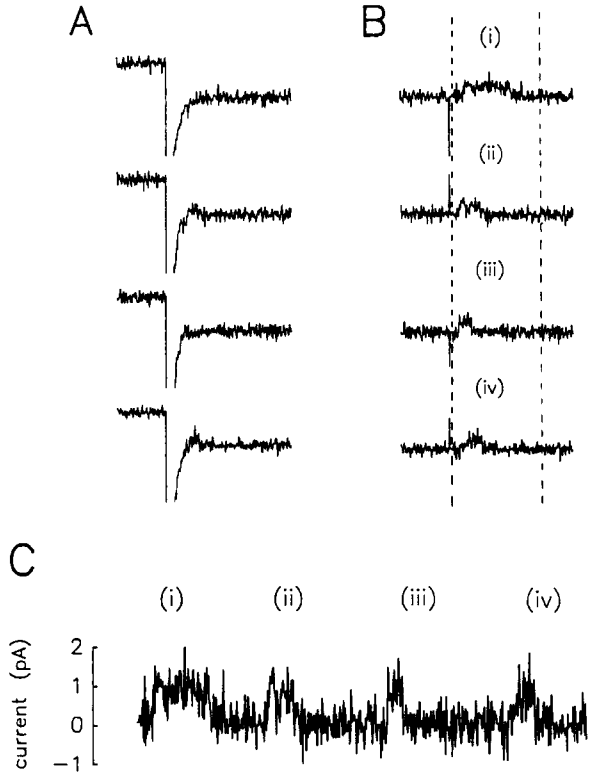

Fig. 1. Illustration of the analysis technique. Shown in (A) are four traces of the original current records obtained when a voltage step from −150 mV to −50 mV was applied repeatedly across a membrane patch. Subtraction of the capacitative transient template yielded the traces in (B). The sections of these records between the dotted lines were then excised and appended to a concatenated data file, an section of which is shown in (C). This data file was then analysed using HMM techniques.

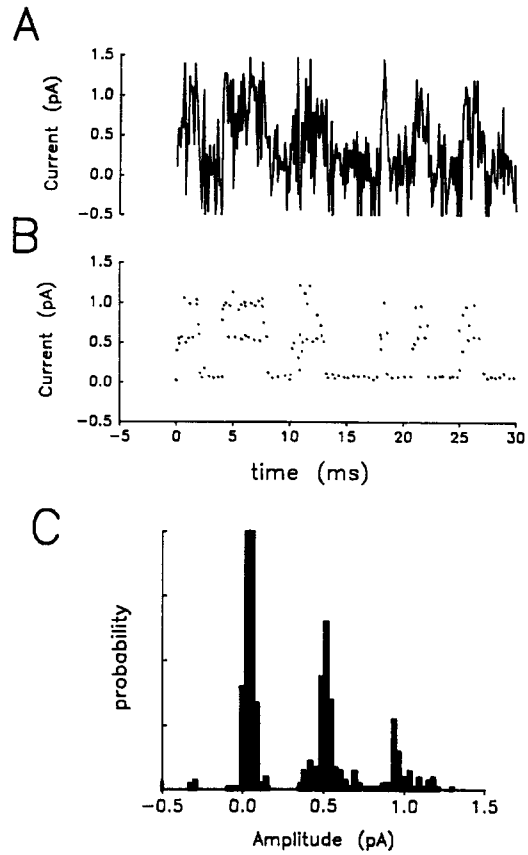

Fig. 2. HMM analysis of the data. A section of a concatenated data file is shown in (A). Displayed in (B) is there sulting maximum a posteriori signal estimate, which shows the most likely underlying signal level at each sample point (data was sampled at 10 kHz). This MAP estimate can be expressed as a histogram, as shown in (C). Obvious peaks are present at around 0.5 pA and 0.9 pA, as well as the baseline peak at just above zero.

Fig. 2B. The MAP signal sequence is the most likely estimate of channel currents embedded in the original noisy trace, given the assumptions that the signal is a 100-state, first-order Markov chain, the noise is Gaussian and the signal and noise are uncorrelated. With this quantization, channel amplitudes can be resolved with a resolution of 40 fA. To deduce the amplitude of the single channel, we constructed an amplitude histogram of the MAP estimate, shown in Fig. 2C. The peak at the left-hand side at just above 0 pA represents the baseline, whereas those to the right around 0.5 pA and 0.9 pA represent the amplitude of open channel currents, which are due to the opening of either only one channel or two channels simultaneously. In this instance the estimate of single-channel current was therefore 0.48 pA, with two channels being active in the patch.

This analysis in a total of 12 patches gave an estimate of the elementary pore conductance of 5.27 ± 0.17 pS.

3.2. Decomposition of multiple channels

Several analytical schemes exist which enable one to deduce the kinetics of individual ion channels from trans-

membrane currents which originate from the collective behaviour of many channels that open and close intermittently. We have applied the procedure detailed elsewhere [14] to estimate the amplitude and the kinetics of single channels from a current trace that contained the activity of many single channels. This analytical method also enables us to deduce whether channels activated by a step change in the transmembrane potential open and close independently of each other or if their gating behaviour is in partial synchrony.

As an illustration of the technique, let us suppose that there are two identical channels, each of which opens and closes according to its individual transition probability matrix **A**. If the two channels are totally independent, one will observe a three-state signal sequence with the 3×3 transition probability matrix $\boldsymbol{A}_I$:

$$\boldsymbol{A}_I = \boldsymbol{L}(\boldsymbol{A} \otimes \boldsymbol{A})\boldsymbol{R} \tag{1}$$

where $\otimes$ denotes the tensor product and $\boldsymbol{L}$ and $\boldsymbol{R}$ are aggregation matrices. On the other hand, the matrix of the two combined channels that are totally coupled can be written as:

$$\boldsymbol{A}_C = \begin{pmatrix} \zeta & 0 & 1-\zeta \\ 1-\delta & 0 & \delta \\ 1-\rho & 0 & \rho \end{pmatrix} \tag{2}$$

where ζ is the probability that the channel remains closed at time $t+1$ given that it was closed at time t, whereas ρ is the probability that the channel stays open at time $t+1$ given that it was open at time t. The bias probability δ ensures that the coupled chain is either fully open or closed. When the constituent channels are neither fully coupled nor totally independent, the matrix of such a partially-coupled vector chain can be defined as:

$$\boldsymbol{A}_{PC} = \kappa \boldsymbol{A}_C + (1-\kappa)\boldsymbol{A}_I, \quad 0 \le \kappa \le 1 \tag{3}$$

where κ is the coupling factor. The equation means that: (i) whenever κ is near 0, the channels open and close essentially independently; (ii) whenever κ is near 1, the channels open and close together as a group; and (iii) for values of κ between 0 and 1, the channels have a tendency to open and close in groups although at times they may seem to act independently. The above equations can readily be extended for the summed currents from L identical channels.

Given real sets of measurements, the parameters in Eqs. (1), (2) and (3) can be estimated by minimizing the set $\Theta = \{\zeta, \rho, \kappa\}$ such that

$$\begin{aligned} \Theta &\equiv \arg\min_{\Theta} \tfrac{1}{2}\|\boldsymbol{A}(\Theta) - \hat{\boldsymbol{A}}\|_F^2 \\ &= \arg\min_{\Theta} \tfrac{1}{2} \sum_{i=0}^{L} \sum_{j=0}^{L} \left(a_{ij}(\Theta) - \hat{a}_{ij}\right)^2 \\ &= \arg\min_{\Theta} \mathcal{J}(\Theta) \end{aligned} \tag{4}$$

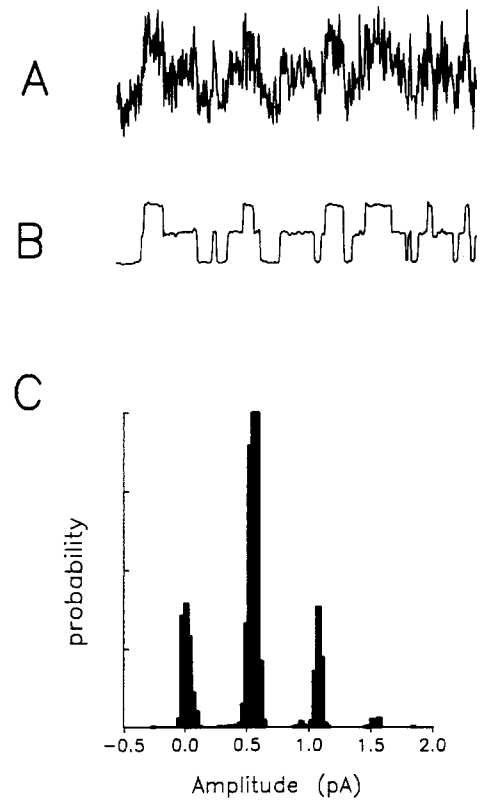

Fig. 3. The decomposistion of multiple channels. A segment of a data file with the MAP signal estimate are shown in (A) and (B), respectively. Clearly defined current levels can be seen at around 0.5 pA and 1.1 pA. These levels were also very obvious in the histogram derived from this MAP estimate as shown in (C). Although transitions to a third open level cannot be seen in (B), these did occur occasionally as evidenced by the small peak around 1.6 pA in the histogram. This data was obtained at 5°C with 280 mM sodium in the pipette.

where $\|\cdot\|$ is the Frobenius norm of a matrix. The elements $\hat{a}_{ij}$ of the transition matrix $\hat{\boldsymbol{A}}$ can be estimated from the HMM processing method. Loosely stated, the strategy is to find numerical values of the three parameters (namely, ζ, ρ, κ) such that the difference between the calculated matrix $\boldsymbol{A}$ using Eq. (3) and the matrix $\hat{\boldsymbol{A}}$ estimated from the real data will be minimized. A simple adaptive procedure utilizing a gradient of descent strategy has been developed to estimate ζ, ρ and κ iteratively so as to minimize the cost function $\mathcal{J}(\Theta)$ [14].

The results of such an analysis of real data from a membrane patch are shown in Fig. 3. A short segment of the original concatenated data file is shown in Fig. 3A and the MAP estimate of the signal sequence is displayed in Fig. 3B, drawn in this case such that transitions between the current levels can be seen. For clarity, this data was recorded from a patch held at a temperature of 5°C, in order to slow the kinetics and reveal transitions more clearly. The concentration of sodium ions in the solution was increased to 280 mM, in order to increase the single-channel current. Co-incidentally, this combination of temperature and ion concentration gives a single-channel conductance similar to that at room temperature with 140 mM

sodium. A histogram derived from the estimated signal sequence revealed four clear peaks, one at 0 pA (representing the baseline), and the others at 0.55, 1.11 and 1.60 pA. Having thus ascertained that the channel currents could adopt one of the three open levels, we wish to determine whether the 0.55 pA level is a subconductance of a channel whose fully-open current level is 1.11 pA. To answer this question, we estimated a 4×4 transition probability matrix, under the assumption that the signal contained in the noisy trace was a first-order, 4-state Markov chain. The allowed state levels were specified as 0, 0.55, 1.11 and 1.60 pA. The estimated transition probability matrix obtained from the 10000-point record read:

$$A = \begin{pmatrix} 0.89 & 0.11 & 0.00 & 0.00 \\ 0.04 & 0.95 & 0.01 & 0.00 \\ 0.00 & 0.06 & 0.93 & 0.01 \\ 0.00 & 0.00 & 0.08 & 0.92 \end{pmatrix} \quad (5)$$

The first entry of the first row of the matrix represents the probability that the process remained in the closed state at time $t+1$ given that it was closed at time t, whereas the second entry of the first row represents the probability of transiting to the 0.55 pA level at time $t+1$ given that it was closed at time t. The zeros in the last two entries of the first row indicate that the transition from the closed state to the 1.11 pA level or the 1.60 pA level never occurred. Conversely, the last row of the matrix shows that transition from the 1.60 pA level to the closed level or the 0.55 level never occurred. In other words, the three channels opened and closed totally independently of each other.

3.3. Determination of coupling coefficient

By substituting the matrix given in Eq. (5) for $\hat{A}$ in Eq. (4), we obtained the value of the coupling coefficient κ to be, as expected, zero, and the transition probability matrix A of the single channel. Although we derive the coupling coefficient to be zero, one can occasionally find in the record seemingly instantaneous transitions from the closed state to the second current level. Such an example can be seen in the segment of the data illustrated in Fig. 3.

In practice membrane patches seldom contained only one or two channels, but usually many channels opened in a given patch in response to a step change of the membrane potential. The analytical scheme outlined above can readily be extended to such records.

Fig. 4A shows a segment of a concatenated data file from a patch which contained many active channels. The maximum current amplitude in response to a step in membrane potential often exceeded 4 pA. The amplitude distribution for the entire data record is shown, aligned with the data record, in Fig. 4B. No information about the amplitude of single channels or the number of active channels contained in the patch could be gleaned from this skewed amplitude histogram. However, clearly defined current levels can be discerned from the amplitude distribution estimated with the HMM processing technique (Fig. 4D). The 10 identifiable peaks in the histogram are separated by 0.62 ± 0.02 pA, suggesting that the multiple channels contained in the patch had identical conductance levels. (The actual values are 0.65, 0.655, 0.705, 0.605, 0.655, 0.608, 0.56, 0.608, 0.56.) These current levels were then used to produce the maximum likelihood estimate of the signal sequence shown in Fig. 4C. From this analysis, we deduced that the maximum current level is derived from the sum of 9 single-channel currents. It can be seen from the MAP estimate that when the channels opened in response to the change in membrane potential, they did not do so in a perfect synchrony. Similarly, the channels closed in steps, as indicated by the stepwise decay of the currents from the peak level. The transition probability matrix for this data read:

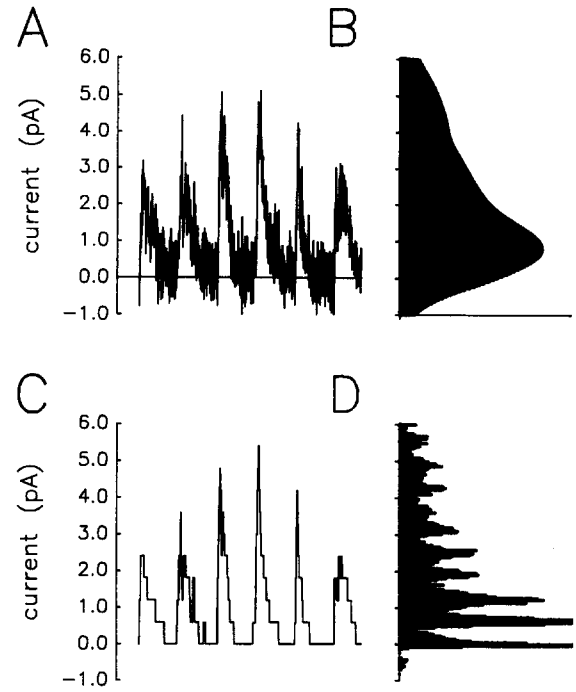

Fig. 4. Analysis of data from a membrane patch containing many channels. Shown in (A) is a section of the data file recorded from a cell attatched patch in response to a potential step from −150 mV to −50 mV. The all-points amplitude distribution derived from this data is shown in (B), which is aligned with the data record. After processing, the histogram shown in (D) was produced. Regularly spaced peaks can be seen with an interval of 0.62 pA. These clearly defined current levels were then used to produce the maximum a posteriori signal estimate shown in (C).

$$A = \begin{pmatrix} 0.96 & 0.01 & 0.03 & & & & & & & \\ 0.05 & 0.93 & 0.02 & & & & & & & \\ & 0.07 & 0.84 & 0.04 & 0.03 & 0.02 & & & & \\ & & 0.14 & 0.80 & 0.05 & 0.01 & & & & \\ & & & 0.15 & 0.71 & 0.14 & & & & \\ & & & 0.01 & 0.14 & 0.67 & 0.18 & & & \\ & & & & & 0.28 & 0.61 & 0.11 & & \\ & & & & & & 0.12 & 0.76 & 0.12 & \\ & & & & & & & 0.31 & 0.62 & 0.07 \\ & & & & & & & & 0.44 & 0.56 \end{pmatrix} \quad (6)$$

For clarity, the zeros in the matrix are left blank. Let us consider the second row as an example of the way the matrix is interpreted. The figure 0.93 is the probability that the current level remains at the lowest open state (the 0.62 pA level) at time $t + 1$ given that it is at this level at time t. Similarly, the figure 0.05 is the probability that the current level will drop to the next lowest level (the baseline level in this example) at time $t + 1$ whereas the figure 0.02 is the probability that it will increase to the next highest level at time $t + 1$. Inspection of this transition probability matrix shows that the current record underwent transitions almost exclusively between neighbouring states. The coupling coefficient κ as defined in Eq. (3) for this patch was close (but not identical) to zero ($\kappa = 0.012$).

Analysis of this type was repeated for data obtained with different step potentials for many different membrane patches and the values of coupling coefficients obtained from 10 patches were then averaged. The mean coupling coefficient κ was 0.03 ± 0.01. We therefore conclude that sodium channels contained in the membrane patch are virtually uncoupled in that they open and close predominantly independently of each other.

3.4. The estimation of mean open duration

The transition probability matrix deduced from solving Eqs. (3) and (4) also gives the mean channel open duration. Using the same notation as in Eq. (2), the mean open duration is related to ρ by:

$$\bar{d}_o = \frac{1}{1-\rho} \tag{7}$$

Here the duration is expressed as the number of sample points and hence it must be multiplied by the sampling interval to obtain a measurement in seconds. For example, from the matrix given in Eq. (5) we deduce that the transition probability matrix of each of the three independent channels is:

$$\boldsymbol{A} = \begin{pmatrix} 0.972 & 0.028 \\ 0.027 & 0.973 \end{pmatrix} \tag{8}$$

Thus, the mean open duration of this channel is calculated to be $1/(1 - 0.973) = 37$ or 3.7 ms, since the sampling interval was 100 μs. Note that this was obtained at 5°C. Similarly, the decomposition of the matrix given in Eq. (6) gives the transition probability matrix of single channels contributing to the summed current as:

$$\boldsymbol{A} = \begin{pmatrix} 0.991 & 0.009 \\ 0.054 & 0.946 \end{pmatrix} \tag{9}$$

The mean open duration of single channels at room temperature thus is calculated to be 0.93 ms. The estimates of mean open time ranged from 0.5 ms at 31°C to 5.6 ms at 4°C. Also, at a give temperature, it depended to a lesser extent on the applied voltage step. We will report elsewhere a rigorous measurement of mean single-channel open time, determined using this procedure, and the effect of changes in membrane potential and ambient temperature.

3.5. Linearity of the current–voltage relationship

In addition to the coupling coefficient and mean channel open time, our analysis yielded accurate measurements of the amplitude of single-channel currents at different membrane potentials.

A single-channel current–voltage relationship obtained from one typical patch is shown in Fig. 5A. To construct this figure, we first obtained 100 records each of channel activity in response to several different potential steps in

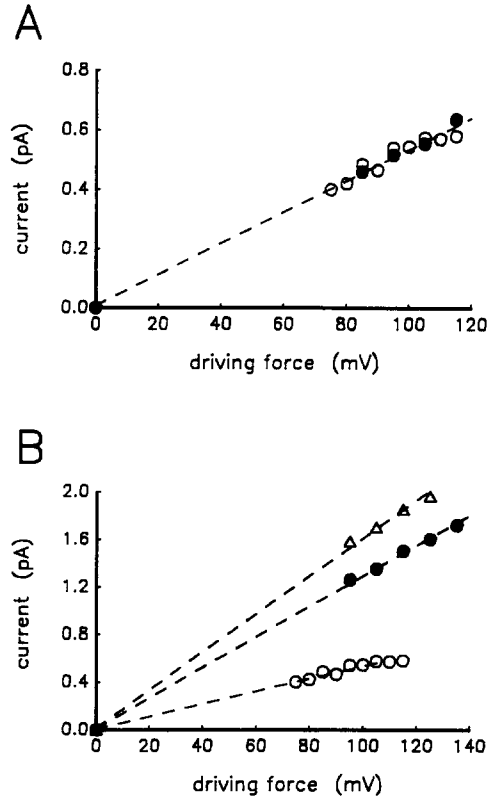

Fig. 5. Current–voltage relation for single-channel currents. Open circles in (A) show data from an inside-out patch plotted as single-channel current vs. the electrochemical driving force on the sodium ion (namely, the membrane potential at which the currents were recorded minus the equilibrium potential for sodium ions, calculated from sodium ion concentrations across the membrane). The dotted line is the regression line through the data points (constrained to pass through the origin). This line has a slope of 5.3 pS. The filled circles show data from the same patch of membrane in cell attatched configuration, with the driving force calculated assuming an intracellular sodium ion concentration of 10 mM. In (B) the open circles are the same inside out patch data illustated in (A). The filled circles show data from an experiment in which the sodium ion concentration on the extracellular side of the membrane was increased to 280 mM, keeping the temperature at 20°C. The slope of the regression line through the data is 11.1 pS. When the temperature of the same patch was raised to 25°C, the data shown by the open triangles was obtained. The conductance was increased to 16.3 pS and the current–voltage relation remained linear.

cell-attached configuration. The single-channel current amplitudes were then measured for each potential. Immediately after collecting this data, we pulled the patch from the cell, thus converting it to inside-out configuration, and repeated the measurements. The open circles in Fig. 5A show data obtained in the inside-out configuration, where the Nernst potential for sodium ions can be calculated from the known concentrations of sodium ions on either side of the membrane. The single-channel current is plotted against the electrochemical driving potential on sodium ions. The line shows a linear regression through the data points which is also constrained to pass through the origin. This line has a slope of 5.3 pS, a conductance virtually identical to the mean of 12 patches examined. The closed circles show the data for the same patch in cell-attached configuration. In this case the Nernst potential is, of course, unknown, but the data fitted the same line as that obtained in the inside out configuration if we assume an intracellular concentration of sodium ions of 10 mM. The single-channel conductance (as shown by the regression line) was 5.3 pS for both patch configurations (room temperature). Note that the single-channel current varied linearly with the ionic electrochemical potential, namely, the channel obeyed Ohm's law over the range of potentials studied.

Measurements of single-channel currents over a larger range of potentials were not possible, unfortunately, since at membrane potentials more negative than about -60 mV the channels failed to activate, and at potentials more depolarised than about $+10$ mV the channel kinetics became too fast to analyze. Nevertheless, it is of considerable interest whether or not the channel current may saturate as the driving potential is increased. To resolve this question, we increased the sodium ion concentration and raised the bath temperature. Fig. 5B shows current voltage relationships for single-channel currents in another patch with the extracelluar sodium ion concentration increased from 140 mM to 280 mM and with the temperature increased to 25°C. When the sodium concentration was doubled, the currents also approximately doubled at all potential steps (filled circles). When the temperature was increased from 20°C to 25°C, with the pipette sodium concentration kept at 280 mM, the current amplitude further increased by about 47%. In all three cases, the single channel continued to obey Ohm's law. This result was found consistently, in 12 patches examined.

4. Discussion

Various values have been quoted in the literature for the conductance of cardiac sodium channels. A confounding factor in most estimates, however, is the uncertainty regarding conductance substates, and again a variety of different conclusions can be found as to the number and magnitude of such substates [15,16]. However, most techniques for the analysis of current records have relied upon visual measurement of channel open time and current. This is an extremely difficult task when several simultaneously active channels are present in a membrane patch, especially when the kinetics of channel activation and inactivation are unmodified. To circumvent this problem many investigators have used agents which remove sodium channel inactivation. It is not known whether or not this treatment changes other channel properties such as conductance level and possibly the factor governing the coupling between the adjacent channels (e.g., [8,5]). Here we have used a digital signal processing technique which yields an unambiguous measure of single-channel conductance. This technique makes possible the accurate determination of single sodium channel properties even when the gating of the channels is unmodified and when there are many channels in the membrane patch.

Typically, the standard deviation of the background noise, when the output of a patch-clamp amplifier is filtered at 10 kHz, is about 0.5 pA, nearly the same as the amplitude of single-channel currents. When the data contain such a large noise component relative to the signal, a small change in channel currents, due for example to a change in the driving force, can only be ascertained accurately with the aid of a signal processing technique such as the one we used. The signal processing technique based on hidden Markov model rests on two key assumptions. Firstly, the noise contaminating the record is Gaussian and white and is uncorrelated with the signal. Secondly, the signal can be represented as a *homogeneous* (i.e., stationary in time), *first-order*, finite-state Markov process. Neither of these assumptions are strictly met in our records of voltage-gated sodium channels. The power spectrum of the patch-clamp amplifier noise, instead of being flat, increases at high frequency (i.e., the noise is not white). Moreover, the opening and closing of a single voltage-gated sodium channel cannot be construed as a homogeneous, first-order Markov process, since the transition probabilities are changing rapidly in time. However, although these assumptions simplify the derivation of the re-estimation formulas and the implementation of the processing algorithm, departure of the data from the idealized signal model does not affect the reliability of the estimation method. For further discussion, see [9,10].

From our analysis of voltage-gated cardiac sodium channels, we draw three salient conclusions. First, a unitary conductance of this channel is 5.3 ± 0.2 pS at room temperature. Second, the current amplitude increases as an integral multiple of the unitary current level and the coupling between several unitary active channels in the patch is weak. Finally, the current–voltage relationship of a unitary channel obeys Ohm's law.

An accurate estimate of the conductance level will prove to be of great importance in understanding the molecular mechanisms underlying the permeation of ions through a membrane channel. Once the height of the

energy barrier is estimated by means of, for example, the temperature-dependence of the conductance, an accurate measure of the conductance value itself will enable us to deduce the radius of the constricted region of the open pore and roughly estimate the geometry of the transmembrane ionic channels. The conductance value we provide here is, we feel, the most accurate one currently available in the literature. It is broadly similar to the conductances that most other workers ascribe to subconductance states of the channel [17,18].

Is the lowest conductance level of 5.3 pS a conductance substate of a channel whose open level is 10.6 pS or 15.9 pS or is it a unitary channel conductance? Generally, the criterion used when inferring that one level is a conductance substate of another is that one can find examples of synchronous openings and asynchronous closings or vice versa. In contrast, we modelled the signal obtained from a current record as being due to the simultaneous activity of an unknown number of elementary conducting pores, each of which is represented as a binary Markov process. Using the mathematical formulation given in Eq. (3), we then derived the numerical value of a parameter which we call the coupling coefficient, which gives a measure of the degree to which the channels are behaving independently. This measure is analogous to the correlation coefficient, in that one variable can be correlated, uncorrelated, or partially correlated with another. Since the coupling coefficient we measure for sodium channels is not exactly zero, one can occasionally find examples of current levels jumping from the closed state to the 10.6 pS level. However, far more usually the transition from one current level to another is between adjacent levels, as if individual channels open and close essentially independently of each other.

The single-channel current–voltage relationship is ohmic, and the conductance increased monotonically with increasing ionic concentration and increasing temperature. Contrary to reports suggesting that the cardiac sodium channel exhibits a change in conductance with voltage [2], we observed a linear relationship over a wide range of potentials. In addition we find that the channel is far from saturated at physiological ion concentrations, since doubling the sodium concentration increases the conductance by two fold, and increasing the temperature increases the conductance still further. At 30°C with 280 mM Na in the extracellular medium, the amplitude of channel current reached 2.45 pA when the driving potential was 135 mV. Thus, the channel was capable of processing about $1.5 \cdot 10^7$ ions per second, more than 3.5 times the processing rate at 20°C in physiological salt concentration. The findings that the channel obeys Ohm's law and does not show saturation or rectification (at near to physiological ion concentrations) greatly simplifies the model of ion permeation.

Acknowledgements

This work was in part supported by grants from the Ramaciotti Foundations and the National Health and Medical Research Council of Australia. Present address of M.K.P. is the Department of Pharmacology and Therapeutics, University of British Columbia, Vancouver, B.C., Canada. B.C. Medical Services Foundation scholar.

References

[1] Cachelin, A.B., De Peyer, J.E., Kokubun, S. and Reuter, H. (1983) J. Physiol. Lond. 340, 389–401.
[2] Kunze, D.L., Lacerda, A.E., Wilson, D.L. and Brown, A.M. (1985) J. Gen. Physiol. 86, 691–719.
[3] Patlak, J.B. and Ortiz, M. (1985) J. Gen. Physiol. 86, 89–104.
[4] Scanley, B.E. and Fozzard, H.A. (1987) Biophys. J. 52, 489–495.
[5] Schreibmayer, W. and Jeglitsch, G. (1992) Biochim. Biophys. Acta 1104, 233–242.
[6] Albitz, R., Droogmans, G. and Nilius, B. (1991) Gen. Physiol Biophys. 10, 3–9.
[7] Albitz, R., Droogmans, G. and Nilius, B. (1991) Biochim. Biophys. Acta 1068, 254–256.
[8] Correa, A.M., Latorre, R. and Bezanilla, F. (1991) J. Gen. Physiol. 97, 605–625.
[9] Chung, S.H., Moore, J.B., Xia, L., Premkumar, L. and Gage, P.W. (1990) Phil. Trans. R. Soc. Lond. B 329, 265–285.
[10] Chung, S.H., Krishnamurthy, V. and Moore, J.B. (1991) Phil. Trans. R. Soc. Lond. B 334, 357–384.
[11] Gage, P.W. and Chung, S.H. (1994) Proc. R. Soc. Lond. B 255, 167–172.
[12] Vasudevan, S., Premkumar, L., Stowe, S., Gage, P.W., Reiländer, H. and Chung, S.H. (1992) FEBS Lett. 311, 7–11.
[13] Farmer, B.B., Mancina, M., Williams, E.S. and Watanabe, A.M. (1983) Life Sci. 33, 1–18.
[14] Kennedy, R.A. and Chung, S.H. (1992) Proc. IEEE Conf. on Decision and Control 4, 3529–3543.
[15] Kohlhardt, M. (1990) Am. J. Physiol. 259, C599–C604.
[16] Schreibmayer, W., Tritthart, H.A. and Schindler, H. (1989) Biochim. Biophys. Acta 986, 172–186.
[17] Nilius, B., Vereecke, J. and Carmeliet, E. (1989) Pflügers Arch. 413, 242–248.
[18] Patlak, J. (1988) J. Gen. Physiol. 92, 413–430.